Electrical Properties of Nanocomposites Based on Comb-Shaped Nematic Polymer and Silver Nanoparticles

Natalia A. Nikonorova,*,† Evgeny B. Barmatov,‡ Dmitry A. Pebalk,§ Marina V. Barmatova,|| Gustavo Domínguez-Espinosa,⊥ Ricardo Diaz-Calleja,⊥ and Polycarpos Pissis#

Institute of Macromolecular Compounds of the Russian Academy of Sciences, Bolshoi pr. 31, St. Petersburg, 199004 Russia, Department of Chemistry, Moscow State University Moscow, 119992 Russia, LG Chem, Moscow Technology Center, Krasnopresnenskaya Nab 12, Moscow, 123610 Russia, Boreskov Institute of Catalysis, Pr. Akademika Lavrentieva, 5, Novosibirsk, 630090 Russia, Department of Applied Thermodynamics ETSII, Polytechnic University of Valencia 46022, Valencia, Spain, and Department of Physics, National Technical University of Athens, 15780 Athens, Greece

Received: December 18, 2006; In Final Form: April 23, 2007

A nematic comb-shaped copolymer and its nanocomposites containing 0.063−0.54 in vol % of silver nanoparticles were studied by broadband dielectric spectroscopy. The frequency dependence of specific alternating current (ac) conductivity was used to estimate the temperature-frequency intervals of charge transfer by long and short distances, respectively. With increasing the concentration of nanoparticles, specific ac conductivity increases. The concentration dependence of dielectric permittivity suggests that distribution of nanoparticles is homogeneous, and conducting channels are not formed. With increasing the concentration of silver nanoparticles, the glass transition temperature of the nanocomposites, described in terms of the strength/fragility concept, increases, whereas the strength parameter D decreases (i.e., "fragility" increases).

Introduction

Liquid crystal (LC) polymers are acknowledged to be fascinating objects from the viewpoint of both modern chemistry of macromolecular compounds and materials science because of the unique combination of their properties: molecular and dynamic characteristics of low-molecular mass liquid crystals on the one hand and important physicomechanical properties of polymer compounds on the other hand.[1] In this respect, the synthesis and characterization of nanocomposites based on LC polymers present a challenging and high-priority task. Investigation of these nanocomposites not only allows one to design various multifunctional "smart" materials, but also makes it possible to understand the nature and the mechanisms of influence of nanoparticles on the development and stability of mesophases.[2−4]

Special attention has been paid to studying the electrical properties of LC nanocomposites, as this investigation allows one to gain important information concerning the mechanism of various processes at the molecular scale and to outline the areas of their possible practical application (in optics, for the development of advanced membrane materials, sensors, etc.).

The electrical properties of nanocomposites can be explored by various methods including dielectric spectroscopy. This method makes it possible to study, in addition to dipolar polarization/relaxation, the molecular mechanism of conductivity and to ascertain the nature of charged particles involved in charge transfer (ions, holes, protons, etc.). In addition to dipolar polarization/relaxation data, analysis of conductivity data allows one to obtain a deeper insight into the mechanism of molecular mobility related to reorientation of polar kinetic units and transfer of free charges. Electric conductivity measurements are also crucial for the estimation of frequency and temperature intervals corresponding to the reliable performance of various devices based on LC nanocomposite materials.

The results of dielectric spectroscopy measurements are treated within the framework of various functions (formalisms). This description involves the analysis of various frequency dependences for the following functions: complex dielectric permittivity $\epsilon^* = \epsilon' - i\epsilon''$, complex electric modulus $M^* = M' + iM''$, complex impedance $Z^* = Z' - iZ''$, complex admittance $Y^* = Y' + iY''$, and complex specific conductivity $\sigma^* = \sigma' + i\sigma''$. All the above functions are interrelated because $\epsilon^* = 1/M^*$, $\epsilon^* = Y^*/iC_0$, $Z^* = 1/Y^*$, $\epsilon^* = \sigma^*/i\epsilon_0\,\omega$ ($\omega = 2\pi f$ is the angular frequency, C_0 is the capacity of measuring cell, and ϵ_0 is the permittivity of vacuum).[5,6]

The proper choice of formalism makes it possible to reveal various details and aspects of electrical and dielectric behavior for a given system under certain temperature-frequency experimental conditions. For example, relaxation of dipole polarization, as provided by the temperature-induced reorientation of polar kinetic units, is usually described by the complex dielectric permittivity ϵ^*. At the same time, processes related to the motion of charge carriers are better described by the complex electric modulus M^*, the complex impedance Z^* and the complex specific conductivity σ^*. In particular, when conductivity is studied by dielectric spectroscopy the frequency dependence of the real part of complex specific conductivity, σ^*, is often considered because this dependence allows one to estimate the specific direct current (dc) conductivity σ_{dc}.

In this work, we studied hybrid polymer systems based on a LC polymer matrix containing silver nanoparticles. More specifically, the nematic comb-shaped LC copolymer P of the

* Corresponding author. E-mail: n_nikonorova2004@mail.ru. Tel.: +7-812-3288535. Fax: +7-812-3286869..

† Institute of Macromolecular Compounds of the Russian Academy of Sciences.

‡ Moscow State University Moscow.

§ Moscow Technology Center.

|| Boreskov Institute of Catalysis.

⊥ Polytechnic University of Valencia.

National Technical University of Athens.

10.1021/jp068688a CCC: $37.00
Published on Web 05/31/2007

SCHEME 1: Chemical Structure of the Copolymer P

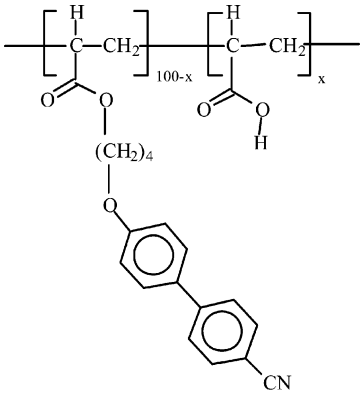

TABLE 1: Diameter of Ag Nanoparticles and Phase Transition Temperatures of Polymer P and of the Nanocomposites[a]

sample	diameter of nanoparticles, nm	phase transition temperatures, °C
P		G 37 N 96 I (1,3[b])
P−Ag (0,063)	5	G 53 N 93 I (1,1)
P−Ag (0,128)	8	G 59 N 87 I (0,7)
P−Ag (0,259)	11	G 60 I
P−Ag (0,54)	16	G 61 I

[a] G is glassy state, N is nematic phase, and I is isotropic phase. [b]Enthalpy of isotropization, J/g, is shown in parentheses.

chemical structure shown in Scheme 1 with mesogenic cyanobiphenyl side groups (70 mol %) and functional units of acrylic acid ($X = 30$ mol %) was used as polymer matrix. Polymer nanocomposites were then prepared by thermal reduction of silver ions in the presence of the LC polymer.[2] To study the effect of the concentration of silver nanoparticles on the electrical properties of the nanocomposites, functions of ϵ^*, σ^*, and M^* were analyzed and compared.

Experimental Methods

Nanocomposites were prepared from nematic polymer P (Scheme 1) with weight-average molecular mass equal to 9300 and polydispersity index equal to 1.4. They are designated by P−Ag (y), where y gives the volume fraction of nanoparticles. Table 1 presents for copolymer P and the nanocomposites the phase transition temperatures, glass transition temperature and isotropization temperature (according to the differential scanning calorimetry (DSC) measurements), and the mean dimensions of the nanoparticles (estimated by transmission electron microscopy, TEM). Synthesis of the copolymer P and the P−Ag nanocomposites, as well as the physicochemical characteristics of the nanocomposites containing different amounts of silver nanoparticles, were reported in detail in refs 2, 3. To a solution of LC polymers P in freshly distilled absolute tetrahydrofuran, a calculated amount of the salt (1,5-cyclooctadiene)(hexafluoroacetylacetonato)silver(I) (Aldrich) was added. The mixture was stirred for 2 h with a magnetic stirrer, dried at room temperature, and was held at 95 °C for 7 days at atmospheric pressure and then for 24 h in vacuum. In this work, we focus on the investigation of the electrical characteristics of the nanocomposites with different volume content (y) of silver nanoparticles varying from 0.063 to 0.54%.

Dielectric measurements were performed using the frequency response analyzer FRA 1260 (Novocontrol) in the interval of frequencies $10^{-2}-10^{7}$ Hz and of temperatures from 20 to 160 °C. The temperature of the sample was controlled with accuracy better than ± 0.1 K. The sample capacitor consisting in two stainless steel electrodes was filled with the polymer at temperatures above the clearing temperature. A constant sample thickness of 50 ± 1 μm was maintained by the use of silica spacers. The diameter of the potential electrodes was 10−20 mm.

The morphology of synthesized nanoparticles was observed on a JEOL TEM-2010 transmission electron microscope (TEM). The samples were mounted on standard copper grids precoated with collodion or Formvar thin films (100−200 nm) and were observed at an accelerating voltage of 60−120 kV.

Results and Discussion

Polymer nanocomposites were prepared according to the procedure based on the thermal reduction of silver ions in the presence of LC polymers.[2,3] On the TEM micrograph (Scheme 2) one can see that nanoparticles mainly have a sphere shape and they are characterized by a certain size distribution. The increase in silver concentration in LC polymer matrix is accompanied by the growth of nanoparticles sizes (Table 1). The influence of the content of silver nanoparticles on the clearing (melting of LC phase) and glass transition temperatures of nanocomposites are shown in Table 1. The formation of nanoparticles in nematic polymer matrix P leads to increase of the glass transition and significant decrease of the clearing temperature. As the result, the overall mesophase stability is rapidly decreasing. It is remarkable that the complete disruption of mesophase is observed at very low (~0.259 vol %) content of silver nanoparticles. Further increase of metal content does not lead to any significant changes in phase behavior of composites. The glass transition keeps the same value, and composites P−Ag are amorphous.

The above experimental data shows that the presence of metal nanoparticles may have a marked effect on the temperature range of the mesophase and on the glass transition temperature. This behavior is related to the adsorption of functional polymer groups on the surface of silver nanoparticles. Two basic types of interaction between LC polymer and silver nanoparticles are proposed as shown in Scheme 2. First includes the chemosorption of CN groups on the surface of silver nanoparticles and concomitant formation of the σ-complex.[2] It should also be taken into account that macromolecules are capable of adsorption on the nanoparticles via the dipole−dipole mechanism (owing to the interaction of carboxylic groups of copolymers P with the surface of nanoparticles).[3]

1. Frequency Dependences of ϵ', ϵ'', tgδ, and σ'_{ac}. All studies were performed at high temperatures where the measured dielectric properties are primarily controlled by charge-transfer processes. Under such conditions, conductivity is the main factor contributing to dielectric characteristics, whereas contribution from dipolar polarization and relaxation can be neglected.

In the rubbery state (or in other words at $T > T_g$), all polymers studied in this work show similar trends in the frequency dependence of real ϵ' and imaginary part ϵ'' of complex dielectric permittivity ϵ^*, as well as of $tg\delta = \epsilon''/\epsilon'$. As an example, Figure 1a−c presents results for the frequency dependence of ϵ', ϵ'', and $tg\delta$, respectively, for polymer P at several temperatures. The values of ϵ', ϵ'', and $tg\delta$ at low frequencies and high temperatures are seen to increase by several orders of magnitude, as compared with the corresponding values characterizing dipolar polarization processes and are typical of conductivity relaxation and space-charge polarization. The above processes are ensured by charge migration between the surface of electrodes and test sample.[7,8] At lower temperatures and

SCHEME 2: TEM Image of Compound P−Ag (0,54) and Schematic Representation of Various Modes of Interaction between Macromolecules of an LC Polymer P and the Surface of Silver Nanoparticles[2,3]

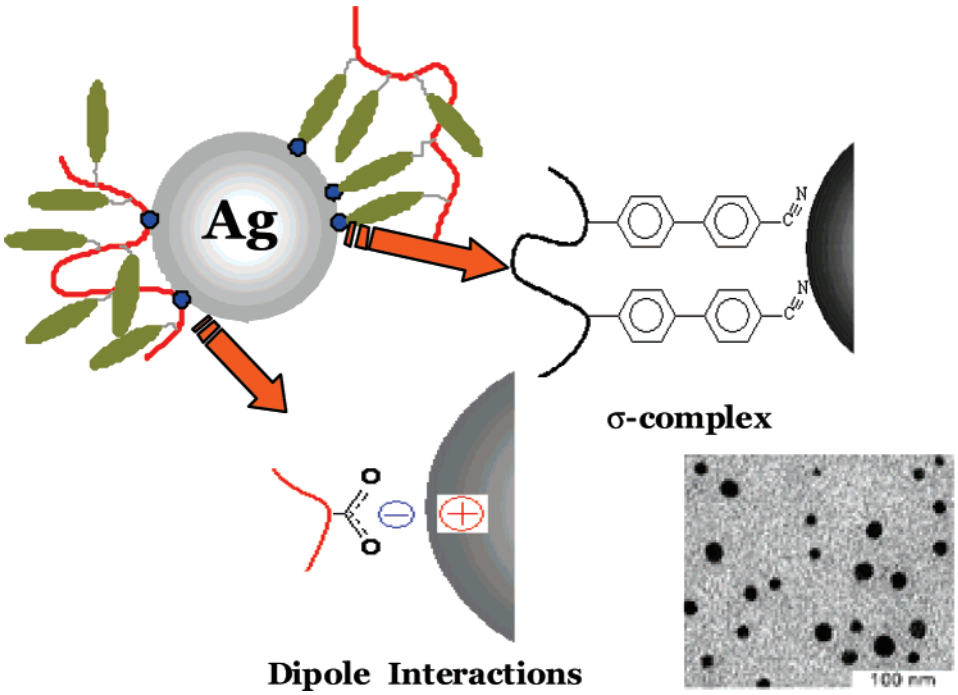

higher frequencies, dipolar polarization/relaxation processes are observed (e.g., a loss peak in Figure 1b at 10^1-10^2 Hz at 70 °C shifting to higher frequencies with increasing temperature). The investigation of these dipolar processes is beyond the scope of this work.

In addition to conductivity relaxation and space-charge polarization, high values of ϵ', ϵ'', and $tg\delta$ in the low-frequency/high-temperature regions can be provided by the so-called Maxwell−Wagner−Sillars (MWS) polarization and relaxation, which are observed in systems with microphase separation.[9] The MWS polarization is afforded by the polarization in the bulk of the sample at the interfacial boundary between two phases with different values of conductivity and dielectric permittivity. Because of the high conductivity of Ag nanoparticles, the characteristic frequency of relaxation of the MWS polarization (MWS relaxation) of the individual (isolated) Ag nanoparticles is in the GHz frequency region[9] (i.e., outside the range of dielectric measurements in this work). However, one can hardly exclude the fact that at a certain concentration of Ag nanoparticles these are able to form aggregates of various sizes in the polymer matrix, which include also a fraction of polymer, and this behavior can entail further microphase segregation. Charge carriers could then be trapped in the region of the aggregates, giving rise to MWS polarization/relaxation in the frequency/temperature regions of study in this work. In the following, we focus on that point and provide further evidence that conductivity relaxation and space-charge polarization rather than MWS polarization/relaxation are at the origin of the effects observed at low frequencies and high temperatures in Figure 1.

In the case of the MWS polarization/relaxation, the corresponding frequency dependence of ϵ'' shows a maximum and that of ϵ' a step (with high increment of dielectric permittivity $\Delta\epsilon = 10-20$, which is independent of temperature). With increasing temperature, peak and step are shifted to higher frequencies.[10] One can see that the frequency dependences of ϵ' and ϵ'' in Figure 1a,b, respectively, do not reflect the specific features of the MWS polarization/relaxation. However, this could be explained by the fact that the relaxation process due to the MWS polarization is masked by high values of ϵ'' and ϵ' in the low-frequency/high-temperature regions.

To further follow the question as to whether MWS polarization/relaxation is responsible for the increase in ϵ', ϵ'', and $tg\delta$ in Figure 1 in the low-frequency/high-temperature regions, let us consider the frequency dependence of specific alternating current (ac) conductivity σ'_{ac}. Similar to the other systems under study, the plot $\log\sigma'_{ac} = \varphi(\log f)$ of polymer P in Figure 2 shows well-pronounced plateau regions at low frequencies, which extend to higher frequencies with increasing temperature and which can be associated with the free-charge transfer in the rubbery state.[11] The σ'_{ac} values in the plateau region correspond to the dc conductivity σ_{dc} The transition from the plateau region to the frequency dependence of σ'_{ac} (at frequency f^*) corresponds to the change in the mechanism of electrical conduction.[11,12] In this case, the plateau region in the left-hand part of the dependence $\log\sigma'_{ac} = \varphi(\log f)$ describes the movement of charges by long distances; in the right-hand part, σ'_{ac} increases with increasing frequency, and the motion of charged carriers is spatially limited within their potential wells.

The frequency regions of σ_{dc} in Figure 2 correspond to that of ϵ'' high values in Figure 1b. In the low-frequency/high-temperature regions, all systems under study are characterized by linear dependences $\log \epsilon'' = \varphi(\log f)$ with slopes close to −1. For example, for polymer P and P−Ag (0.54) the slope of the linear dependence $\log \epsilon'' = \varphi(\log f)$ at 130 °C is equal to −0.98. As was shown earlier, this behavior is typical of conductivity relaxation.[9,13] Therefore, one can expect that the dramatic growth in dielectric losses shown in Figure 1b is associated with dc conductivity and there is no contribution arising from MWS polarization/relaxation.

In the lowest-frequency/highest-temperature intervals, the frequency dependences of ϵ'' (Figure 1b), $tg\delta$ (Figure 1c), and σ'_{ac} (Figure 2) show the following features: deviation from the linear character of ϵ'', maximum of $tg\delta$, and slight decrease in the σ'_{ac} values. The above features of dielectric behavior are typical of electrode polarization, associated with the accumula-

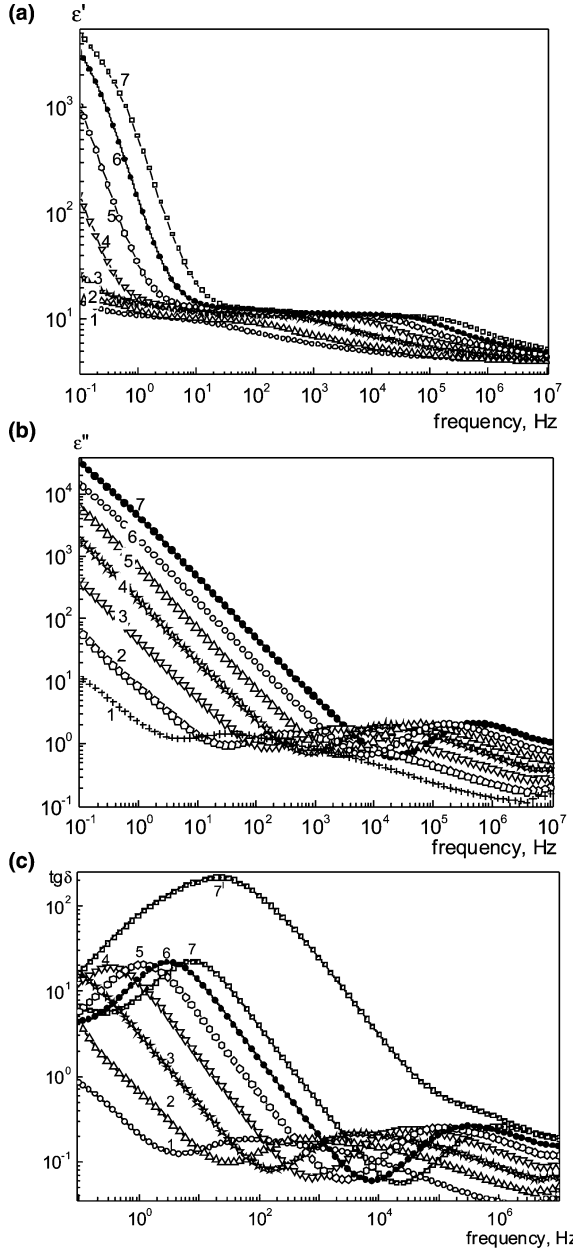

Figure 1. Frequency dependence of ϵ' (a), ϵ'' (b), and $tg\delta$ (c) for polymer P at temperatures 70 °C (1), 80 °C (2), 90 °C (3), 100 °C (4), 110 °C (5), 120 °C (6), and 130°C (7) and of $tg\delta$ for P−Ag (0,54) at 130 °C (7′).

tion of charges at the interfaces between the electrodes and the polymer sample.[6,11,14−16]

2. Temperature Dependences of Specific Conductivity. For many polymers, the experimental dependence of specific conductivity (as well as of dipole relaxation times) on reciprocal temperature in the softening regions are described by the empirical Vogel−Tammann−Fulcher−Hesse (VTFH) equation[11,17,18]

$$\sigma_{dc} = \sigma_{dc0} \exp[-B/(T - T_0)] \quad (1)$$

where σ_{dc0}, B, and T_0 are fitting parameters; T_0 is the so-called Vogel temperature, which is lower than the glass transition temperature by several tens of degrees, typically around 50 °C.

Figure 3 presents the dependences log $\sigma_{dc} = \varphi(1/T)$ for polymer P and the P−Ag nanocomposites approximated through eq 1. As it is clearly observed, all the above dependences are

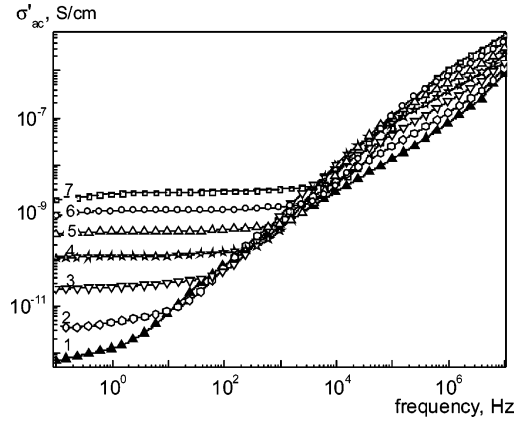

Figure 2. Frequency dependence of σ'_{ac} for polymer P at temperatures 70 °C (1), 80 °C (2), 90 °C (3), 100 °C (4), 110 °C (5), 120 °C (6), and 130 °C (7).

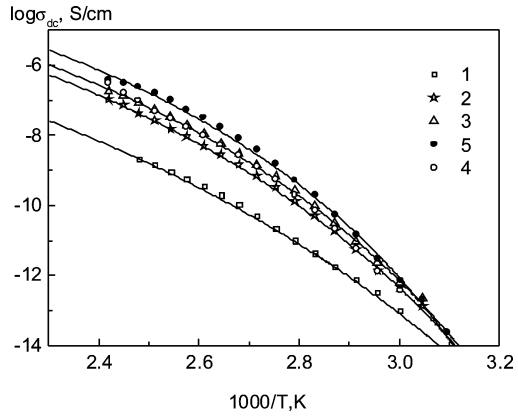

Figure 3. Dependence of log σ_{dc} on reciprocal temperature for P (1), P−Ag (0,063) (2), P−Ag (0,128) (3), P−Ag (0,259) (4), and P−Ag (0,54) (5). Full lines are best fittings of eq 1 to the experimental data.

well described by the VTFH equation (solid lines). This fact suggests that in the systems under study conductivity in low-frequency/high-temperature ranges is controlled by the segmental mobility of chains. (Below the glass transition temperature, when segmental mobility is frozen, the dependences log $\sigma_{dc} = \varphi(1/T)$ are linear.[16,19])

The temperature dependence of specific dc conductivity is often described in terms of the strength/fragility concept.[20] In this case, the VTFH equation is modified as

$$\sigma_{dc} = \sigma_{dc0} \exp[-DT_0/(T - T_0)] \quad (2)$$

where D is the so-called strength parameter. The D value is a measure of fragility.

The fragility concept was introduced to take into account both thermodynamic and kinetic aspects of glass transition. The parameter D characterizes the deviation of the temperature dependence log $\sigma_{dc} = \varphi(1/T)$ from the Arrhenius linear dependence. The lower the D values, the higher the deviation of the dependence log $\sigma_{dc} = \varphi(1/T)$ from its linear character. For example, for "strong" systems, including ionic glasses, the D values are high and achieve 100, and the dependences log $\sigma_{dc} = \varphi(1/T)$ are almost linear. For covalent glasses, D approaches 30. Polymers are known to be fragile systems, and their D values are equal to 5−20.[20,21]

On the other hand, deviation of the temperature dependences of conductivity σ_{dc} (or relaxation times of dipole polarization) from their linear character in the region of the α-process suggests that the above relaxation process shows a well-pronounced

TABLE 2: Parameters of the VTFH from Eq 2 for Polymer P and the P−Ag Nanocomposites Obtained from the Curves in Figure 3 and Glass Transition Temperature T_g Determined from Eq 3

sample	log σ_{dc0}, S/cm	T_0, K	D	T_g, °C
P	−0.9	211	16.4	26
P−Ag (0,063)	−0.27	234	11.9	32
P−Ag (0,128)	−0.33	241	10.5	33
P−Ag (0,259)	−0.46	250	9.4	37
P−Ag (0,54)	−0.31	252	8.8	35

cooperative character. This means that the movement of such charge carriers depends on the state of polymer matrix and on the nearest neighborhood. Cooperative motion proceeds as a joint correlated drift of numerous charge carriers together with polymer chains. As to the local motion of particles, this is treated as a single motion from one energy equilibrium state to another, and this displacement is independent of neighborhood.

The parameters log σ_{dc0}, D, and T_0 of eq 2 for P and P−Ag are summarized in Table 2. We observe that with increasing concentration of nanoparticles D decreases (i.e., "fragility" increases). This fact implies that with increasing the concentration of nanoparticles their effect on polymer matrix becomes more pronounced and the charge transfer in the nanocomposites (conductivity relaxation process) becomes more cooperative.

Knowing the parameter D, one can estimate the glass transition temperature T_g, as both values are related by the following empirical expression[17,22]

$$T_g = T_0(1 + 0.0255D) \quad (3)$$

Table 2 presents the glass transition temperature calculated through eq 3. As it is observed, by introduction of only 0.063 vol % of silver nanoparticles the glass transition temperature increases by 6 °C. As the concentration of silver nanoparticles is further increased, the glass transition temperatures remain virtually unchanged. It is interesting to note that similar trends of T_g changes with concentration of silver nanoparticles are observed for the T_g values obtained from the dielectric data (Table 2) and from the DSC (Table 1), although absolute values and steps of increase are higher in the case of DSC.

Calculation of glass transition temperatures through eq 3 seems to be rather simple and reliable. This approach can be used even when high values of conductivity do not allow one to estimate relaxation time values, τ_{max}, for the α-process from the frequency dependence of ϵ'' (which is the usual way to determine T_g by dielectric spectroscopy) or when the DSC curves are so diffuse that correct estimation of glass transition temperature T_g is impossible.

3. The Effect of the Concentration of Silver Nanoparticles on the Specific Conductivity and Dielectric Permittivity of Nanocomposites. Figure 4 shows results for the frequency dependence of σ'_{ac} for polymer P and the nanocomposites at 120 °C. The following observations can be made. First, with increasing the concentration of silver nanoparticles the frequency plateau is extended to higher frequencies (on passing from copolymer P to P−Ag (0.54), the frequency of transition from dc to ac conductivity, f^*, increases by 1 order of magnitude). Second, the σ_{dc} values tend to increase with increasing the concentration of silver nanoparticles.

Figure 5 (curve 1) demonstrates the dependence of σ_{dc} on concentration of silver nanoparticles. One can see that for the nanocomposites with the highest silver content, P−Ag (0.54), σ_{dc} increases by 2 orders of magnitude as compared to that of the initial copolymer P. However, even for P−Ag (0.54) the

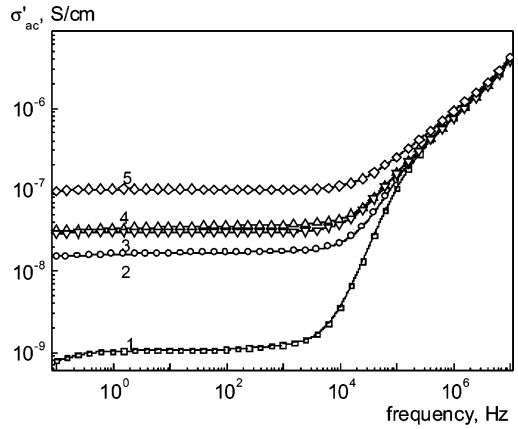

Figure 4. Frequency dependence of σ'_{ac} for P (1), P−Ag (0,063) (2), P−Ag (0,128) (3), P−Ag (0,259) (4), and P−Ag (0,54) (5) at 120 °C.

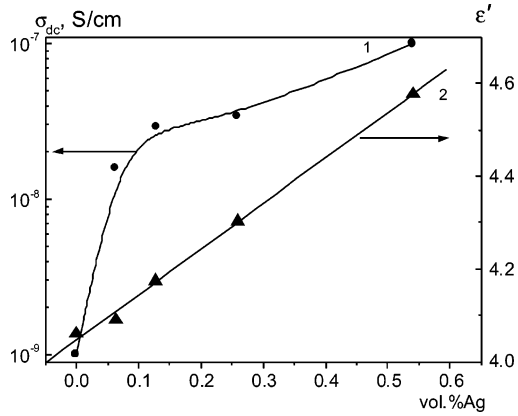

Figure 5. Dependence of σ_{dc} at 120 °C and of ϵ' at 60 °C (f = 10 kHz) on concentration of silver nanoparticles.

σ_{dc} value is still low and typical for polymer dielectrics rather than for percolating systems. Although the highest concentration of silver in the nanocomposites is much lower than the theoretical percolation threshold of about 16 vol % for a statistical distribution of spherical particles in a three-dimensional system,[23,24] it is worth to further follow the question as to the origin of dc conductivity in Figure 4. The reason for that is that in many practical systems the experimental values of percolation threshold are much lower than the theoretical one, owing to specific distributions of the conducting filler in aggregates, chains, etc.[25] Coming back to Figure 4, the rather low values of dc conductivity imply that in the nanocomposites the individual nanoparticles are enveloped in the polymer matrix, and there are no jumps of charge carriers (electrons) from one nanoparticle to another (in other words, no percolation bridges are formed). In the opposite case, introduction of silver nanoparticles should be accompanied by a sharp increase in conductivity (by 3−7 orders of magnitude).[23−25] Further evidence for that will be provided later.

Thus, analysis of $\log\sigma'_{ac} = \varphi(\log f)$ in Figure 4 allows one to estimate σ_{dc} at different experimental conditions and to determine the limits of the conductivity mechanism when charge carriers can be transferred by short and long distances. As indicated above, conductivity is due to ions in the polymer matrix rather than due to electrons of the silver nanoparticles. Further support for that is coming from the temperature dependence of dc conductivity in Figure 3. The VTFH dependence is in support of a conductivity mechanism governed by the motion of the polymeric chains, as typically observed in polymers at temperatures higher than T_g.[9]

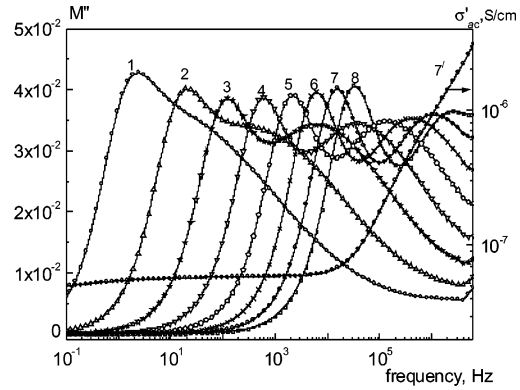

Figure 6. Frequency dependence of M'' (1−8) and of σ'_{ac} (7′) for P−Ag (0,128) at 70 °C (1), 80 °C (2), 90 °C (3), 100 °C (4), 110 °C (5), 120 °C (6), 130 °C (7,7′), and 140 °C (8).

Let us consider now the effect of the concentration of silver nanoparticles on the dielectric permittivity of P−Ag nanocomposites. This study seems to be important from the viewpoint of practical applications, such as for the preparation of dielectrics with increased values of dielectric permittivity for capacitors, and also for finding the proper route of controlled synthesis of nanocomposites with desired characteristics.

To understand the effect of metal concentration on the dielectric permittivity of nanocomposites, experimental conditions (frequency and temperature) should be selected so that the contributions from space-charge polarization and conductivity relaxation are negligible, and the properties of nanocomposites are controlled by their chemical nature. For all systems under study, the above conditions are the following: temperature is 60 °C, and frequency is 10 kHz.

Figure 5 (curve 2) presents experimental values of dielectric permittivity at 10 kHz and 60 °C for the P−Ag nanocomposites with different volume concentrations y of silver nanoparticles. As it is seen, in the range $y = 0-0.54\%$, this dependence is virtually linear. We know that in percolation systems the dielectric permittivity below the percolation threshold is described by a fractional power law and increases exponentially with the volume concentration approaching the percolation threshold.[25] Thus, the results in Figure 5 indicate that metal concentrations in the nanocomposites under investigation are far below the percolation threshold. The specific increment of dielectric permittivity $\Delta\epsilon/y$ in Figure 5 is equal to 0.0118. For composites with electronic (metallic) conductivity $\Delta\epsilon/y$ is by, at least, 1 order of magnitude higher.[26,27] Hence, one can expect that the nanocomposites under investigation here are characterized by statistical distribution or, in other words, by rather uniform distribution of nanoparticles in the polymer matrix. In this connection, it is no wonder that such systems do not show any MWS polarization. The relatively low values of dielectric permittivity in Figure 5 allow one to conclude that the volume fraction of nanoparticles are not large enough to ensure the electronic (metallic) type of conductivity in the nanocomposites.

Bearing in mind the evidence provided above that the concentration of silver in the nanocomposites is much below the percolation threshold and that the distribution of nanoparticles is rather uniform, the question arises why dc conductivity in the nanocomposites increases, as compared to the pure copolymer P (Figures 3−5). According to percolation theory, for nanocomposites with metal concentrations far below the percolation threshold the conductivity values should be close to that of the pure matrix.[23−25] On the other hand, the VTFH dependence of conductivity in Figure 3 suggests that in all the samples conductivity arises from ions and is governed by the motion of the polymeric chains and follows a similar kinetics in the nanocomposites and in the pure matrix. The level of conductivity is then determined by concentration and mobility of the ions.

The higher values of dc conductivity in the nanocomposites then have to be attributed to higher concentrations of ions, probably arising as impurities in the preparation process.

4. Complex Electric Modulus. When the dielectric behavior is analyzed by means of complex electric modulus M^*, the contribution from space-charge polarization is minimized. This approach allows one to distinguish dipolar relaxations from the conductivity relaxation.[11,28]

Real and imaginary parts of complex electric modulus M^* are related to dielectric permittivity and loss factor by the following equation:[19]

$$M' = \epsilon'/(\epsilon'^2 + \epsilon''^2)$$
$$M'' = \epsilon''/(\epsilon'^2 + \epsilon''^2)$$

For all systems under study, the frequency dependence of M'' at temperatures above the glass transition temperature shows two well-defined maxima M''_{max}. As an example, Figure 6 presents the dependence $M'' = \varphi(\log f)$ for the P−Ag (0.128) at several temperatures. Two peaks are observed and for both, with increasing temperature, the position of $f_{max,M''}$ is shifted to higher frequencies. This tendency implies that the above processes show relaxation character.

To answer the question concerning the molecular mechanism of the above processes, let us compare the frequency dependences of M'' and σ'_{ac}. At the same temperature, the frequency $f_{max,M''}$ of the first, low-frequency M'' peak is close to f^* for all systems under study (as the illustration compares curves 7 and 7′ in Figure 6). This tendency has been earlier observed for the conductivity relaxation.[11,19] Hence, for the P−Ag nanocomposites the low-frequency peak in Figure 6 can be also attributed to the conductivity relaxation. In this case, the $f_{max,M''}$ values separate the regions of short-range and long-range mobility of charges at the right-hand and left-hand sides of M'' maximum, respectively. The second, high-frequency M'' peak in Figure 6 arises from dipolar relaxation, and its investigation is beyond the scope of this work.

The frequency dependences of the imaginary part M'' of the electric modulus can be described (by analogy with the frequency dependences of ϵ'') by the empirical Havriliak−Negami (HN) model function[19]

$$M^* = \sum_{k=1}^{2} \mathrm{Im}\left\{\frac{\Delta M_k}{(1 + (i\omega\tau_{HNk})^{\alpha})^{\beta}}\right\} \qquad (4)$$

where $\Delta M = M'_\infty - M'_s$, $M'_\infty = 1/\epsilon'_\infty$, and $M'_s = 1/\epsilon'_s$; $\tau = 1/2\pi f$, where f is the frequency of the applied ac electric field; α and β are the calculated shape parameters, which correspond to the widening and asymmetry of relaxation times distribution, respectively; $\tau_{max} = 1/2\pi f_{max}$, where f_{max} is the frequency at which M'' (f) passes through a maximum. The ratio between τ_{max} and τ_{HN} is defined by the following equation:[29]

$$\tau_{max} = \tau_{HN}\left[\frac{\sin\left(\frac{\pi(\alpha_{HN})\beta_{HN}}{2(\beta_{HN}+1)}\right)}{\sin\left(\frac{\pi(\alpha_{HN})}{2(\beta_{HN}+1)}\right)}\right]^{1/(\alpha_{HN})} \qquad (5)$$

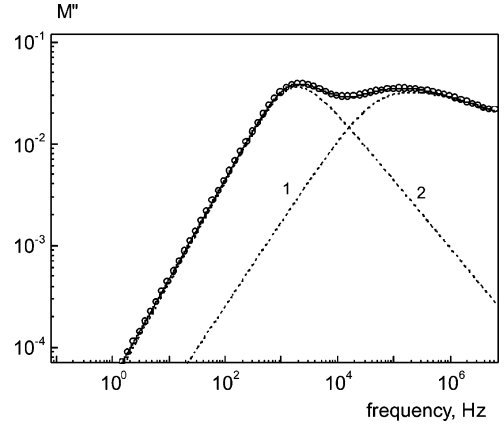

Figure 7. Separation of the frequency dependence of M'' for P−Ag (0,128) at 110 °C into the processes of relaxation of dipole polarization (2) and of conductivity relaxation (1) according to eq 4.

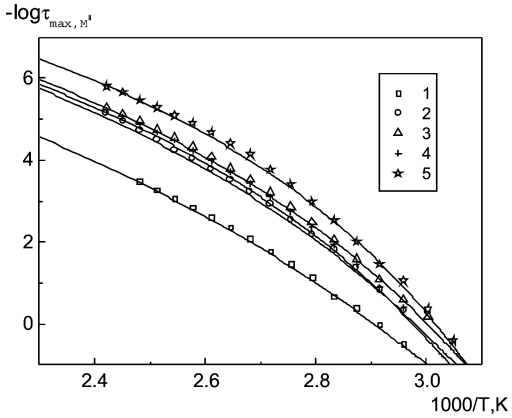

Figure 8. Dependence of log $\tau_{max,M''}$ on reciprocal temperature for P (1), P−Ag (0,063) (2), P−Ag (0,128) (3), P−Ag (0,259) (4), and P−Ag (0,54) (5). Full lines are the best fittings of eq 6 to the experimental data.

For copolymer P and the P−Ag nanocomposites, in the temperature-frequency intervals under study the dependences log $M'' = \varphi(\log f)$ are reliably described by eq 4. As an example, Figure 7 shows the separation of the experimental log $M'' = \varphi(\log f)$ curve for P−Ag (0.128) at 110 °C into two processes, which are provided in the order of increasing frequency by the conductivity relaxation and the relaxation of dipole polarization. For the conductive process, the half-width of the log $M'' = \varphi(\log f)$ curve for P−Ag (0.128) at 110 °C is 1.38; it is higher than that corresponding one to a single Debye peak (1.144). This suggests that the conductive peak includes not only pure ionic contributions but also electrodes polarization effects.[30]

Figure 8 presents the conductivity relaxation times values for P and P−Ag, which were calculated according to eqs 4 and 5. The dependences $\tau_{max,M''} = \varphi(1/T)$ were described by the VTFH equation for the conductivity relaxation times[11,16]

$$\tau_{max,M''} = \tau_{0,M''} \exp[DT_0/(T - T_0)] \quad (6)$$

where $\tau_{0,M''}$, D ($D = B/T_0$), and T_0 have the same meaning as in eqs 1 and 2.

The best-fitting parameters of eq 6 for copolymer P and the nanocomposites are listed in Table 3. As follows from Tables 2 and 3, T_0 and D calculated from the dependences log $\sigma_{dc} = \varphi(1/T)$ (Figure 3) and log $\tau_{maxM''} = \varphi(1/T)$ (Figure 8) appear to be virtually the same (within experimental error) because they reflect the conductivity relaxation processes in the rubbery state and describe the motion of free charges.

TABLE 3: Parameters of the VFTH from Eq 6 for P, P−Ag (0,063), P−Ag (0,128), P−Ag (0,259), and P−Ag (0,54) Obtained from the Curves in Figure 8

sample	log $\tau_{0M''}$, s	B, K	T_0, K	$D = B/T_0$
P	−11.3	3462	211	16.4
P−Ag (0,063)	−11.6	2685	235	11.4
P−Ag (0,128)	−11.4	2416	241	10
P−Ag (0,259)	−11.1	2248	248	9.1
P−Ag (0,54)	−11.1	1876	258	7.3

Conclusions

The LC copolymer P and P−Ag nanocomposites with different concentration of silver nanoparticles were studied by the method of dielectric spectroscopy. Attention was focused on the dielectric behavior at low frequencies in the rubbery state. Under such conditions, contribution to dielectric characteristics is primarily controlled by the conductivity relaxation. Temperature-frequency intervals of charge transfer by long and short distances are estimated from the frequency dependences of σ'_{ac} and of M''.

With increasing the concentration of silver nanoparticles, the specific dc conductivity increases. However, even nanocomposites with high concentrations of silver are far away from the percolation threshold, and no conducting clusters or bridges are formed in these nanocomposites. The concentration dependence of dielectric permittivity suggests a uniform distribution of silver nanoparticles in the polymer matrix, as well as the absence of electronic conductivity.

The dependences log $\sigma_{dc} = \varphi(1/T)$ and log $\tau_{maxM''} = \varphi(1/T)$ are described in terms of the strength/fragility concept, which allows one to estimate the level of cooperativity of the conductivity relaxation process (deviation from the Arrhenius dependence). The results show that with increasing the concentration of metallic nanoparticles, the glass transition temperature, calculated through the strength parameter D, tends to increase.

References and Notes

(1) *Handbook of Liquid Crystals*; Demus, D., Goodby, J., Grey, G. W., Spiess, H. W., Vill, V., Eds.; Wiley VCH: New York, 1998; Vol. I−IV.

(2) Barmatov, E. B.; Pebalk, D. A.; Barmatova, M. V. *Langmuir* **2004**, *20*, 10868.

(3) Barmatov, E. B.; Medvedev, A. S.; Pebalk, D. A.; Barmatova, M. B.; Nikonorova, N. A.; Zezin, S. B.; Shibaev, V. P. *Polymer Sci. A* **2006**, *48*, 665.

(4) Shandryuk, G. A.; Rebrov, A. V.; Vasiliev, R. B.; Dorofeev, S. G.; Merekalov, A. S.; Gas'kov, A. M.; Talroze, R. V. *Polymer Sci. B* **2005**, *47*, 266.

(5) Jonscher, A. K. *Dielectric Relaxation in Solids*; London: Chelsea Dielectrics, 1983.

(6) *Impedance Spectroscopy*; Macdonald, J. R., Ed.; New York: Wiley, 1987.

(7) Kyritsis, A.; Pissis, P.; Grammatikakis, J. *J. Polym. Sci., Polym. Phys. Ed.*. **1995**, *33*, 1737.

(8) Dominguez, L.; Meyer, W. H.; Wegner, G. *Makromol. Chem., Rapid Commun.* **1987**, *8*, 151.

(9) Hedvig, P. *Dielectric Spectroscopy in Polymers*; Adam Hilger: Bristol, England, 1977.

(10) Tsonos, C.; Apekis, L.; Viras, K.; Stepanenko, L.; Karabanova, L.; Sergeeva, L. *Solid State Ionics* **2001**, *143*, 229.

(11) Pissis, P.; Kyritsis, A. *Solid State Ionics* **1997**, *97*, 105.

(12) Yamamoto, K.; Hamikawa, H. *Jpn. J. Appl. Phys., Part 1* **1988**, *27*, 1845.

(13) Bottcher, C. J. F.; Bordewilk, P. *Theory of Electric Polarization*, 2nd edition; Elsevier: Amsterdam, 1978; Vol. 2.

(14) Raistric, I. D. In *Impedance Spectroscopy*; Macdonald, J. R., Ed.; Wiley: New York, 1987; Chapter 2.

(15) Miyairi, K. *J. Phys. D* **1986**, *19*, 1973.
(16) Neagu, E.; Pissis, P.; Apekis, L. *J. Appl. Phys.* **2000**, *87*, 2914.
(17) Polizos, G.; Shilov, V. V.; Pissis, P. *Solid State Ionics* **2001**, *145*, 93.
(18) Jaeckle, J. *Rep. Prog. Phys.* **1986**, *49*, 171.
(19) Neagu, E.; Pissis, P.; Apekis, L.; Gomes Ribelles, J. L. *J. Phys. D: Appl. Phys.* **1997**, *30*, 1551.
(20) Angell, C. A. *J. Non-Cryst. Solids* **1991**, *13*, 131−133.
(21) Boehmer, R.; Ngai, K. L.; Angell, C. A.; Plazek, D. J. *J. Chem. Phys.* **1993**, *99*, 4201.
(22) Angell, C. A. *Annu. Rev. Phys. Chem.* **1992**, *43*, 693.
(23) Zallen, R. *The Physics of Amorphous Solids*; Wiley: New York, 1983.
(24) Stauffer, D.; Aharony, A. *Introduction to Percolation Theory*; Taylor & Francis: London, 1992.
(25) Kotsilkova, R.; Fragiadakis, D.; Pissis, P. *J. Polym. Sci., Part B: Polym. Phys.* **2005**, *43*, 522.
(26) Parnas, Ya.M.; Lebedev, K. I. *Phisica dielectricov* (Physics of dielectrics); AN SSSR: Moscow, 1960.
(27) Sazhin, B. I. *Electritcheskiye svoystva polimerov* (Electrical properties of polymers); Chimiya: Moscow, 1970.
(28) Jain, H.; Ngai, K. L. In *Relaxation in Complex Systems*; Ngai K. L., Wright G. B., Eds.; Naval Research Laboratory: Washington, DC, 1984; 221.
(29) Diaz-Calleja, R. *Macromolecules* **2000**, *33*, 8924.
(30) Kremer, F. In *Broadband Dielectric Spectroscopy*; Schönhals, A., Ed.; Springer-Verlag: Berlin, 2003; Chapter 3.